Bimetallic Transition Metal Complexes of 2,3-Dihydroxy-N'1,N'4-bis((2-Hydroxynaphthalen-1-yl)Methylene) Succinohydrazide Ligand as a New Class of Bioactive Compounds; Synthesis, Characterization and Cytotoxic Evaluation

Abdou S. El-Tabl[1]*, Moshira M. Abd-El Wahed[2], Mohammed A. Wahba[3], Mohamad M. E. Shakdofa[3,4], Asia Gafer[1]

[1]Department of Chemistry, Faculty of Science, El-Menoufia University, Shebin El-Kom, Egypt. [2]Department of Pathology, Faculty of Medicine, El-Menoufia University, Shebin El-Kom, Egypt. [3]Department of Inorganic Chemistry, National Research Centre, P.O. 12311, Dokki, Cairo, Egypt. [4]Department of Chemistry, Faculty of Sciences and Arts, University of Jeddah, Khulais, Saudi Arabia.

ABSTRACT

New series of homobimetallic Cu^{II}, Ni^{II}, Co^{II}, Mn^{II}, Fe^{III}, Zn^{II}, Cd^{II}, Pb^{II} complexes of 2,3-dihydroxy-N'1,N'4-bis((2-hydroxynaphthalen-1-yl)methylene)succinohydrazide have been prepared and analytically and spectroscopically characterized by elemental and thermal (differential thermal analysis and thermal gravim analysis) analyses, infrared (IR), ultraviolet-visible spectra, magnetic moments,^{1}H-nuclear magnetic resonance, mass spectra, molar conductance, and electron spin resonance (ESR) measurements. The analytical and spectral data show that the dihydrazone ligand behaves as a neutral, monobasic or dibasic hexadentate ligand bonded to the metal ions through enolic or ketonic carbonyl oxygen atoms, azomethine nitrogen atoms and protonated or deprotonated naphthanolic hydroxyl oxygen atoms adopted either tetrahedral, square planer or tetragonally distorted octahedral geometries. Molar conductance in dimethylformamide solution indicates that the complexes are non-electrolytes. The ESR spectra of solid Cu^{II} complexes (9-10) and 12 show axial type indicating a $d_{(X2-y2)}$ or $d_{(Z2)}$ ground state with significant covalent bond character. However, Mn^{II} complex (2) and Cu^{II} complex (11) show isotropic type. Cytotoxic evaluation of the ligand and its complexes has been carried out. Complexes show enhanced activity as compared to the parent ligand.

Key words: Hexadentate, Succinohydrazide, Dihydrazone, Erythrocyte sedimentation rate, Cytotoxic behavior.

1. INTRODUCTION

The interaction of transition metal ions with biologically active ligands is one of the most wonderful and potentially useful areas of coordination chemistry [1-3]. Metal chelation has promoted a great interest in the present day medicine and chemical investigations [2,4,5]. Recent years witnessed an intensive investigation of the coordination chemistry of hydrazone due to their interesting coordination properties and diverse applications [6-8]. The chemistry of di-hydrazone ligands has received considerable interest due to their versatility as polyfunctional chelating agents toward different metal ions forming homo- or heterobimetallic complexes [9-11]. Dihydrazone ligands are characterized by the presence of two hydrazonic groups (two interlinked nitrogen atoms) which has made it a good polydentate chelating agents that can form different modes of complexes

with transition metals leading to biological [12], analytical, and catalytic applications. For example oxalyl bis(3,4-dihydroxybenzylidene)hydrazone acts as a reagent for the separation and concentration of ZrO^{2+} ions from different water samples using flotation technique while its complexes have a high effect degraded the DNA of eukaryotic completely [13]. The catalytic potential of dinuclear V(IV), Cu(II), Mn(II) and Ti(IV) complexes of dichelating ligands, bis(2-hydroxybenzylidene)oxalo- and bis(2-hydroxybenzylidene) terephthalohydrazide were evaluated for oxidation of hydrocarbons including cycloalkenes, cyclic alkanes and benzyl alcohol using H_2O_2 as terminal oxidant. The titanium complex of bis(2-hydroxy benzylidene)oxalohydrazide showed the best selectivity and activity as catalyst [14]. In-vitro anti-proliferative activity of a series of trisubstituted 3,5-triazine-2,4,6-triyltris(oxy) tris(benzene-4,1-diyl)

tris(methanylylidene)) tri(benzohydrazide) derivatives against human liver carcinoma (HepG2) and human cervix carcinoma (HeLa) cell have been studied. The activity showed that these compounds exhibited lower activity against HeLa cell lines but reasonably moderate *in vitro* cytotoxicity against HepG2 cell lines [15]. VO^{2+}, Mn^{2+}, Co^{2+}, Ni^{2+}, Cu^{2+} and Zn^{2+}, complexes of 2,5-hexanedione bis(isonicotinylhydrazone) have been prepared and characterized by various analytical and spectrophotometric techniques The molecular modeling of the ligand showed intramolecular hydrogen bonding. It behaves as a dibasic, monobasic or neutral tetradentate ligand bonded to the metal ions via enolic or ketoic carbonyl oxygen, azomethine nitrogen atoms. The magnetic moments and electronic spectra of all complexes provide a square-planar square pyramidal octahedral [16]. Heterometallic trinuclear Cu(II) and Zn(II) complexes bis(2-hydroxy-1-naphthaldehyde) oxaloyldihydrazone have been prepared, characterized [17]. The ligand acts as a tetrabasic hexadentate bridging ligand coordinating to the metal center through enolate, naphtholate oxygen atoms and azomethine nitrogen atoms. Chlorido and perchlorato groups function as bridging ligands while nitrato group functions as a monodentate ligand. Metal centers have tetragonally distorted octahedral, octahedral or distorted square-pyramidal stereochemistry. Heterometallic Mn^{2+} and Ru^{3+} complex of bis(2-hydroxynaphthlen-1-yl)methylene) oxaloyldihydrazide has been synthesized and studied using analytical and spectroscopic measurements [18]. Inspired by the interesting results reported in the previous reports, this manuscript is devoted to the preparation of a new dihydrazone hexadentate ligand, namely, 2,3-dihydroxy-$N^{'1},N^{'4}$-bis ((2-hydroxynaphthalen-1-yl)methylene)succinohydrazide (H_6L). The new ligand is designed for metal complexation and the formation of highly stable homobimetalic Cu^{II}, Ni^{II}, Co^{II}, Mn^{II}, Fe^{III}, Zn^{II}, Cd^{II}, Pb^{II}, and Fe^{III} complexes. The ligand and its complexes were characterized using various spectroscopic such as infrared (IR), mass, nuclear magnetic resonance (NMR), electronic absorption and electron spin resonance (ESR) spectra, as well as conductivity and magnetic moment measurements in addition to analytical techniques as elemental and thermal analyses.

2. EXPERIMENTAL
2.1. Materials
All the reagents employed for the preparation of the ligand and its complexes were synthetic grade and used without further purification. Thin layer chromatography (TLC) is used to confirm the purity of the compounds.

2.2. Physical Measurements
The ligand and its metal complexes were analyzed for C, H and N analyses at the Microanalytical Unit, Cairo University Egypt. A standard gravimetric

method was used to determine metal ions [19-21]. All metal complexes were dried under vacuum over P_4O_{10}. The IR spectra were measured as KBr pellets using a Perkin-Elmer 683 spectrophotometer (4000-400 cm^{-1}). Electronic spectra (qualitative) were recorded on a Perkin-Elmer 550 spectrophotometer. The conductance(10^{-3} M) of the complexes in dimethylformamide (DMF) were measured at 25°C with a Bibby conductimeter type MCl.^{1}H-NMR spectra of the ligand and its Cd^{II} complex were obtained with Perkin-Elmer R32-90-MHz spectrophotometer using tetramethylsilane as an internal standard. Mass spectra were recorded using JEULJMS-AX-500 mass spectrometer provided with the data system. The thermal analyses (differential thermal analysis [DTA] and thermal gravim analysis [TGA]) were carried out in air on a Shimadzu DT-30 thermal analyzer from 27 to 800°C at a heating rate of 10°C per minute. Magnetic susceptibilities were measured at 25°C by the Gouy method using mercuric tetrathiocyanato cobalt(II) as the magnetic susceptibility standard. Diamagnetic corrections were estimated from Pascal's constant [22]. The magnetic moments were calculated from the equation: $\mu_{eff} = 2.84\sqrt{\chi_M^{corr} \cdot T}$. The ESR spectra of solid complexes at room temperature were recorded using a varian E-109 spectrophotometer, 2,2-Diphenyl-1-picrylhydrazyl was used as a standard material. The TLC of all compounds confirmed their purity.

2.3. Preparation of the ligand, $(N^{'1},N^{'4})$-2,3-dihydroxy-N'1,N'4-bis((2-hydroxynaphthalen-1-yl)methylene)succinohydrazide
The di-hydrazone ligand, $(N^{'1},N^{'4})$-2,3-dihydroxy-N'1,N'4-bis((2-hydroxynaphthalen-1-yl)methylene) succinohydrazide (H_6L) was prepared by refluxing (1.78 g, 1 mmol) of 2,3-dihydroxysuccinohydrazide dissolved in 40 cm^3 of methanol with (3.44 g, 2 mmol) 2-hydroxy-1-naphthaldehyde dissolved in 40 cm^3 of methanol (Scheme 1). The mixture refluxed for 2 h with stirring. After cooling, the formed solid product filtered off then washed several times with cold methanol and finally dried at room temperature. Ligand
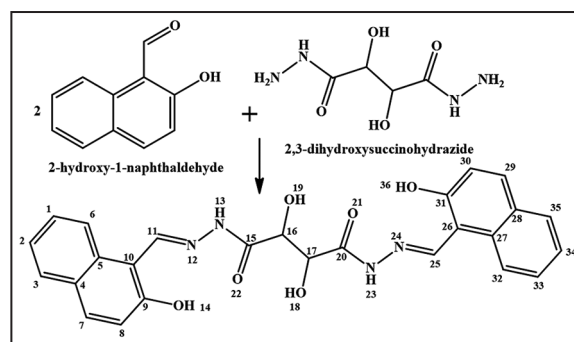
Scheme 1: Preparation of $(N^{'1},N^{'4})$-2,3-dihydroxy-N'1,N'4-bis((2-hydroxynaphthalen-1-yl)methylene) succinohydrazide.

(1): Yield 83%; m.p. >300; color is yellow; Anal. Calcd. for $C_{26}H_{22}N_4O_6$ (FW=486.49): C, 64.19; H, 4.56; N, 11.52. Found (%) C, 63.86; H, 4.75; N, 11.32; IR (KBr, cm^{-1}), 3446,3398 υ(OH), 3315, 3210 υ(NH), 1658 υ(C=O), 1630 υ(C=N), 1288, υ(C-OH[14,36]), 1240 υ(C-OH[18,19]), 988 υ(N-N);^{1}H-NMR (270 MHz, dimethyl sulfoxide [DMSO]-d_6, δ/ppm): 12.95, (s, 2H, OH[14,36]), 9.98 (s, 2H, NH[13,23]), 9.67, (s, 2H, OH[18,19]), 8.88 (s, 2H,[11,25]H-C=N), 7.15-8.10 (m, 12H, aromatic), 4.76 (d, 2H, HOC-C$H^{16,17}$OH). The mass spectrum of the ligand (H_6L) revealed molecular ion peak at m/z 498.

2.4. Metal Complexes (2)-(19) Preparation

The metal complexes 2-19 were prepared by refluxing with string a suitable amount (2 mmol) of a hot ethanolic solution of the following metal salts: $Mn(CH_3COO)_2 \cdot 4H_2O$, $FeSO_4 \cdot 7H_2O$, $CoCl_2 \cdot 6H_2O$, $Co(CH_3COO)_2 \cdot 4H_2O$, $CoSO_4.5H_2O$, $NiSO_4 \cdot 6H_2O$, $Ni(CH_3COO)_2 \cdot 4H_2O$, $Cu(NO_3)_2 2H_2O$, $CuCl_2 \cdot 2H_2O$, $CuSO_4 \cdot 5H_2O$, $Cu(CH_3COO).2H_2O$, $Zn(CH_3COO)_2$. $ZnSO_4.7H_2O$, $CdSO_4 \cdot H_2O$, $Cd(OAc)_2.2H_2O$, $CdCl_2.2H_2O$, $Cd(NO_3)_2.2H_2O$ and $Pb(NO_3)_2 \cdot 2H_2O$ with a hot ethanolic suspension of the ligand (2.43 mg 1 mmol, 30 ml ethanol) in presence or absence of 3 ml of diethyl amine for 4 h respectively. The precipitates which formed were filtered off, washed with ethanol then by diethyl ether and dried in vacuum desiccators over P_4O_{10}. Analytical data for the prepared complexes are:

Complex (2): $[(H_4L)Mn_2(CH_3COO)_2(H_2O)_4].H_2O$: Yield: 65%; m.p. >300°C; color: Beige; molar conductivity (L$_m$): 7.1 ohm^{-1} cm^2 mol^{-1}. Anal. Calcd. (%) for $C_{30}H_{38}N_4O_{15}Mn_2$ (FW=804.5): C, 44.79; H, 4.76; N, 6.98, Mn, 13.69; Found (%) C, 44.15; H, 4.49; N, 7.80, Mn, 13.35; IR (KBr, cm^{-1}), 3433, 3300 υ(OH), 1620 υ(C=N), 1603 υ(N=C-N=C), 1268, υ(C-OH[14,36]), 1241 υ(C-OH[18,19]), 1011 υ(N-N); 650 υ(M-O), 530 υ(M←O), 456 υ(M←N); 1570, 1383 υ$_{sym}$CH$_3$COO, υ$_{asym}$CH$_3$COO (Δ=187 cm^{-1}).

Complex (3), $[(H_4L)Fe_2(SO_4)_2]$: Yield: 75%; m.p. >300°C; color: Dark brown; molar conductivity (Λ$_m$): 23.3 ohm^{-1} cm^2 mol^{-1}. Anal. Calcd. (%) for $C_{26}H_{22}N_4O_{14}S_2Fe_2$ (FW=790.29): C, 39.51; H, 2.81; N, 7.09, Fe, 14.13; Found (%) C, 39.50; H, 3.26; N, 7.41, Fe, 13.97; IR (KBr, cm^{-1}), 3346, 3303 υ(OH), 3270 υ(NH), 1650 υ(C=O), 1617 υ(C=N), 1305, υ(C-O[14,36]), 1244 υ(C-OH[18,19]), 1022 υ(N-N); 605 υ(M←O), 525 υ(M←N)1194, 1141, 830, 665 υ(SO$_4$).

Complex (4), $[(H_2L)Co(H_2O)]$: Yield: 69%; m.p. >300°C; color: Yellow; molar conductivity (Λ$_m$): 9.3 ohm^{-1} cm^2 mol^{-1}. Anal. Calcd. (%) for $C_{26}H_{22}N_4O_7Co$ (FW=561.41): C, 55.62; H, 3.95; N, 9.98, Co, 10.50; Found (%) C, 56.00; H, 4.26; N, 10.41; Co, 10.30; IR (KBr, cm^{-1}), 3320 υ(OH), 1619 υ(C=N), 1579 υ(N=C-N=C), 1319, υ(C-O[14,36]),

1247 υ(C-OH[18,19]), 1021 υ(N-N); 619 υ(M-O), 530 υ(M←O), 500 υ(M←N).

Complex (5), $[(H_4L)Co_2(CH_3COO)_2(H_2O)_4]$: Yield: 55%; m.p. >300°C; color: Brown; molar conductivity (Λ$_m$): 12.3 ohm^{-1} cm^2 mol^{-1}. Anal. Calcd. (%) for $C_{30}H_{32}N_4O_{14}Co_2$ (FW=792.48): C, 45.47; H, 4.32; N, 7.07, Co, 14.87; Found (%) C, 44.99; H, 4.26; N, 7.25.41; Co, 15.01.30; IR (KBr, cm^{-1}), 3406, 3300 υ(OH), 1618 υ(C=N), 1595, υ(N=C-C=N), 1260, υ(C-OH[14,36]), 1245 υ(C-OH[18,19]), 1030 υ(N-N); 657 υ(M-O), 539 υ(M←O), 487 υ(M←N); 1555, 1355 υ$_{sym}$CH$_3$COO, υ$_{asym}$CH$_3$COO (Δ=200 cm^{-1}).

Complex (6), $[(H_6L)Co_2(SO_4)_2]$: Yield: 70%; m.p. >300°C; color: Beige; molar conductivity (Λ$_m$): 33.7 ohm^{-1} cm^2 mol^{-1}. Anal. Calcd. (%) for $C_{26}H_{24}N_4O_{14}Co_2S_2$ (FW=798.48): C, 39.11; H, 3.03; N, 7.02, Co, 14.76; Found (%) C, 40.09; H, 3.26; N, 7.00; Co, 13.92; IR (KBr, cm^{-1}), 3432, 3325 υ(OH), 3280 υ(NH), 1650 υ(C=O), 1623 υ(C=N), 1269, υ(C-OH[14,36]), 1240 υ(C-OH[18,19]), 1006 υ(N-N); 645 υ(M←O), 530 υ(M←O),476 υ(M←N)1184, 1140, 869, 685 υ(SO$_4$).

Complex (7), $[(H_6L)Ni_2(SO_4)_2]$: Yield: 70%; m.p. >300°C; color: Light green; molar conductivity (Λ$_m$): 24.1 ohm^{-1} cm^2 mol^{-1}. Anal. Calcd. (%) for $C_{26}H_{24}N_4O_{14}Ni_2S_2$ (FW=798.00): C, 39.13; H, 3.03; N, 7.02, Ni, 14.71; Found (%) C, 40.12; H, 3.14; N, 7.09; Ni, 15.15; IR (KBr, cm^{-1}), 3433, 3407 υ(OH), 3270 υ(NH), 1656 υ(C=O), 1620 υ(C=N), 1263, υ(C-OH[14,36]), 1242 υ(C-OH[18,19]), 1014 υ(N-N); 618 υ(M-O), 559 υ(M←O),530 υ(M←N);1185, 1122, 832, 669 υ(SO$_4$).

Complex (8), $[(H_4L)Ni_2(CH_3COO)_2(H_2O)_4]$: Yield: 79%; m.p. >300°C; color: Beige; molar conductivity (Λ$_m$): 14.2 ohm^{-1} cm^2 mol^{-1}. Anal. Calcd. (%) for $C_{30}H_{36}N_4O_{14}Ni_2$ (FW=794.01): C, 45.38; H, 4.57; N, 7.06, Ni, 14.78; Found (%) C, 46.55; H, 4.90; N, 7.15; Ni, 14.89; IR (KBr, cm^{-1}), 3455, 3300 υ(OH), 3265 υ(NH), 1645 υ(C=O), 1619 υ(C=N), 1282, υ(C-O[14,36]), 1241 υ(C-OH[18,19]), 1012 υ(N-N); 650 υ(M-O), 581 υ(M←O),534 υ(M←N); 1561, 1383 υ$_{sym}$CH$_3$COO, υ$_{asym}$CH$_3$COO (Δ=178 cm^{-1}).

Complex (9), $[(H_4L)Cu_2(NO_3)_2(H_2O)_4]$: Yield: 80%; m.p. >300°C; color: Light green; molar conductivity (Λ$_m$): 15.7 ohm^{-1} cm^2 mol^{-1}. Anal. Calcd. (%) for $C_{26}H_{30}N_6O_{16}Cu_2$ (FW=809.64): C, 38.57; H, 3.73; N, 10.38, Cu, 15.70; Found (%) C, 40.05; H, 3.90; N, 9.67; Cu, 15.89; IR (KBr, cm^{-1}), 3290 υ(OH), 3275 υ(NH), 1651 υ(C=O), 1620 υ(C=N), 1292, υ(C-O[14,36]), 1244 υ(C-OH[18,19]), 1002 υ(N-N); 530 υ(M-O), 500 υ(M←O), 462 υ(M←N); 1460, 1383, 870, υ(NO$_3$) (Δ=77 cm^{-1}).

Complex (10), $[(H_4L)Cu_2Cl_2(H_2O)_4]$: Yield: 78%; m.p. >300°C; color: Olive; molar conductivity (Λ$_m$): 9.5 ohm^{-1} cm^2 mol^{-1}. Anal. Calcd. (%) for

$C_{26}H_{28}N_4O_{10}Cu_2$ (FW=754.52): C, 41.39; H, 3.74; N, 7.43, Cu, 16.84; Found (%) C, 41.64; H, 3.95; N, 7.00; Cu, 16.10; IR (KBr, cm^{-1}), 3320 υ(OH), 3275 υ(NH), 1648 υ(C=O), 1619 υ(C=N), 1312, υ(C-O[14,36]), 1260 υ(C-OH[18,19]), 1010 υ(N-N); 653 υ(M-O), 550 υ(M←O),511 υ(M←N).

Complex (11), [(H$_2$L)Cu$_2$(H$_2$O)$_2$]**:** Yield: 60%; m.p. >300°C; color: Green; molar conductivity (Λ_m): 72.7 ohm^{-1} cm^2 mol^{-1}. Anal. Calcd. (%) for $C_{26}H_{30}N_6O_{16}Cu_2$ (FW=645.57): C, 48.37; H, 3.43; N, 8.68, Cu, 19.69; Found (%) C, 48.05; H, 3.90; N, 8.67; Cu, 18.89; IR (KBr, cm^{-1}), 3290 υ(OH[18,19]), 1616 υ(C=N), 1589 υ(N=C-C=N), 1331, υ(C-O[14,36]), 1250 υ(C-OH[18,19]), 1026 υ(N-N); 600 υ(M-O), 534 υ(M←O), 499 υ(M←N).

Complex (12), [(H$_6$L)Cu$_2$(SO$_4$)$_2$(H$_2$O)$_4$]: Yield: 85%; m.p. >300°C; color: Light green; molar conductivity (Λ_m): 26.8 ohm^{-1} cm^2 mol^{-1}. Anal. Calcd. (%) for $C_{26}H_{32}N_4O_{18}S_2Cu_2$ (FW=879.77): C, 35.50; H, 3.67; N, 6.37, Cu, 14.45; Found (%) C, 35.05; H, 3.88; N, 6.67; Cu, 14.09 IR (KBr, cm^{-1}), 3433, 3335 υ(OH), 3265 υ(NH), 1654 υ(C=O), 1620 υ(C=N), 1276, υ(C-OH[14,36]), 1255 υ(C-OH[18,19]), 999, υ(N-N); 617 υ(M-O), 555 υ(M←O), 525 υ(M←N);1184, 1118, 832, 670 υ(SO$_4$).

Complex (13), [(H$_4$L)Cu$_2$(CH$_3$COO)$_2$(H$_2$O)$_4$].H$_2$O: Yield: 59%; m.p. >300°C; color: Red brown; molar conductivity (Λ_m): 13.7 ohm^{-1} cm^2 mol^{-1}. Anal. Calcd. (%) for $C_{30}H_{36}N_4O_{15}Cu_2$ (FW=819.72): C, 43.96; H, 4.43; N, 6.83, Cu, 15.50; Found (%) C, 43.05; H, 3.99; N, 6.97; Cu, 15.09; IR (KBr, cm^{-1}), 3290 υ(OH), 3270 υ(NH), 1639 υ(C=O), 1618 υ(C=N), 1299, υ(C-O[14,36]), 1254 υ(C-OH[18,19]), 1011 υ(N-N); 669 υ(M-O), 565 υ(M←O), 530 υ(M←N); 1559, 1383 υ_{sym}CH$_3$COO, υ_{asym}CH$_3$COO (Δ=176 cm^{-1}).

Complex (14), [(H$_4$L)Zn(CH$_3$COO)$_2$]: Yield: 74%; m.p. >300°C; color: Yellow; molar conductivity (Λ_m): 16.2 ohm^{-1} cm^2 mol^{-1}. Anal. Calcd. (%) for $C_{30}H_{28}N_4O_{10}Zn_2$ (FW=735.32): C, 49.00; H, 3.84; N, 7.62, Zn, 17.78; Found (%) C, 49.12; H, 4.00; N, 7.47, Zn, 17.46; IR (KBr, cm^{-1}), 3307 υ(OH), 3278 υ(NH), 1619 υ(C=O), 1604 υ(C=N), 1305, υ(C-O[14,36]), 1241 υ(C-OH[18,19]), 1003 υ(N-N); 616 υ(M-O), 540 υ(M←O), 505 υ(M←N); 1558, 1337 υ_{sym}CH$_3$COO, υ_{asym}CH$_3$COO (Δ=221 cm^{-1}).

Complex (15), [(H$_2$L)Zn(H$_2$O)$_2$]**:** Yield: 65 %; m.p. >300°C; color: Yellow; molar conductivity (Λ_m): 12.5 ohm^{-1} cm^2 mol^{-1}. Anal. Calcd. (%) for $C_{26}H_{26}N_4O_8Zn_2$ (FW=653.27): C, 47.80; H, 4.01; N, 8.58, Zn, 19.66; Found (%) C, 47.56; H, 3.93; N, 8.47, Zn, 19.76. IR (KBr, cm^{-1}), 3390 υ(OH[18,19]), 1621 υ(C=N), 1588 (N=C-C=N), 1312, υ(C-O[14,36]), 1240 υ(C-OH[18,19]), 1001 υ(N-N); 619 υ(M←O), 531 υ(M←N).

Complex (16), [(H$_4$L)Cd$_2$(CH$_3$COO)$_2$]: Yield: 58%; m.p. >300°C; color: Yellow; molar conductivity (Λ_m): 12.8 ohm^{-1} cm^2 mol^{-1}. Anal. Calcd. (%) for $C_{26}H_{22}N_4O_7Cd$ (FW=829.39): C, 43.44; H, 3.40; N, 6.76, Cd, 27.11; Found (%) C, 42.92; H, 3.10; N, 6.27, Cd, 26.46; IR (KBr, cm^{-1}), 3310 υ(OH), 3268 υ(NH), 1655 υ(C=O), 1622 υ(C=N), 1321, υ(C-O[14,36]), 1241 υ(C-OH[18,19]), 1000 υ(N-N); 684 υ(M-O), 571 υ(M←O), 539 υ(M←N); 1566, 1399 υ_{sym}CH$_3$COO, υ_{asym}CH$_3$COO (Δ=167 cm^{-1}).^{1}H-NMR (270 MHz, DMSO-d_6, δ/ppm): 9.85 (s, 2H, NH[13,23]), 9.51, (s, 2H, OH[18,19]), 8.68 (s, 2H,[11,25]H-C=N), 7.0-8.10 (m, 12H, aromatic), 4.88 (d, 2H, CO-CH[16,17]OH), 1.95 (s, 6H, CH$_3$COO).

Complex (17), [(H$_2$L)Cd(H$_2$O)$_2$]: Yield: 76%; m.p. >300°C; color: Yellow; molar conductivity (Λ_m): 14.7 ohm^{-1} cm^2 mol^{-1}. Anal. Calcd. (%) for $C_{28}H_{36}N_4O_{13}Cd$ (FW=743.30): C, 42.01; H, 2.98; N, 7.54, Cd 30.25; Found (%) C, 42.12; H, 2.90; N, 7.67, Cd, 29.46; IR (KBr, cm^{-1}), 3300 υ(OH), 1622 υ(C=N), 1591 υ(N=C-C=N), 1311 υ(C-O[14,36]), 1260 υ(C-OH[18,19]), 1018, 993 υ(N-N); 585 υ(M-O), 548 υ(M←O), 487 υ(M←N).

Complex (18), [(H$_4$L)Cd$_2$(NO$_3$)$_2$]: Yield: 60%; m.p. >300°C; color: Yellow; molar conductivity (Λ_m): 15.1 ohm^{-1} cm^2 mol^{-1}. Anal. Calcd. (%) for $C_{26}H_{22}N_6O_{12}Cd_2$ (FW=835.31): C, 37.38; H, 2.65; N, 10.06, Cd, 26.91; Found (%) C, 37.32; H, 2.90; N, 10.07, Cd, 25.99; IR (KBr, cm^{-1}), 3340 υ(OH), 3270 υ(NH), 1657 υ(C=O), 1622 υ(C=N), 1298, υ(C-O[14,36]), 1244 υ(C-OH[18,19]), 1023, υ(N-N); 617 υ(M-O), 544 υ(M←O), 524 υ(M←N).1433, 1359, 870 υ(NO$_3$) (Δ=74 cm^{-1}).

Complex (19), [(H$_4$L)Pb$_2$(NO$_3$)$_2$]**:** Yield: 89%; m.p. >300°C; color: Yellow; molar conductivity (Λ_m): 35.6 ohm^{-1} cm^2 mol^{-1}. Anal. Calcd. (%) for $C_{26}H_{22}N_6O_{12}Pb_2$ (FW=1024.89): C, 30.47; H, 2.16; N, 8.20, Pb, 40.43; Found (%) C, 30.00; H, 2.00; N, 7.90, Pb, 39.10; IR (KBr, cm^{-1}), 3320 υ(OH), 3275 υ(NH), 1650υ(C=O), 1619 υ(C=N), 1284, υ(C-OH[14,36]), 1243 υ(C-OH[18,19]), 1013, υ(N-N); 653 υ(M-O), 576υ(M←O), 533 υ(M←N);1441, 1362, 850 υ(NO$_3$) (Δ=79 cm^{-1}).

2.5. Biological Activity
2.5.1. Cytotoxic activity
The cytotoxic activity of the ligand and its metal complexes was evaluated *in vitro* against cell lines of *Hep-G2* **(**human liver cancer) and *A-549* (human lung cancer) using the SulfoRhodamine-B-stain (SRB) assay published method in the Pathology Laboratory, Pathology Department, Faculty of Medicine, El-Menoufia University, Egypt [23,24]. Cells were plated in the 96-multiwell plate (10^4 cells/well) for 24 h before treatment with the compounds to allow attachment of cell to the wall of the plate. Different concentrations of the compounds under test in DMSO

(0, 5, 12.5, 25 and 50 μg ml^{-1}) were added to the cell monolayer, triplicate wells being prepared for each individual dose. Monolayer cells were incubated with the complexes for 48 h at 37°C and under 5% CO$_2$. After 48 h cells were fixed, washed and stained with SRB-stain. Excess stain was wash with acetic acid and attached stain was recovered with Tris ethylene-diamine-tetraacetic acid buffer. Color intensity was measured in an enzyme-linked immunosorbent assay reader. The relation between surviving fraction and drug concentration is plotted to get the survival curve for each tumor cell line after addition the specified compound.

3. RESULTS AND DISCUSSION

The ligand, 2,3-dihydroxy-N'^{1}, N'^{4}-bis((2-hydroxynaphthalen-1-yl)methylene)succinohydrazide (H$_6$L) and its metal complexes (2-19) are stable at room temperature, non-hydroscopic and are insoluble in common solvents such as ethanol, acetone, water and chloroform but soluble in DMF and DMSO. The elemental analysis confirmed that all complexes are composed of ligand and metal ions with molar ratios equal to 1L: 2M. Many attempts were made to grow single crystal, but unfortunately, they failed. The analytical, physical and spectral data are presented in experimental part, and Tables 1-3 are compatible with the suggested structures (Figures 1-4).

3.1. The Molar Conductivity

The molar conductivities of 1×10^{-3} M solutions of the metal complexes in DMSO at room temperature were found in the range 7.1-35.6 ohm^{-1} cm^2 mol^{-1} indicating the non-electrolytic nature of all complexes. These low values commensurate the absence of any counters ions in their structure. The considerable high conductance values for some complexes may be due to the partial solvoysis of them [25,26].

3.2. IR Spectra

The IR spectrum of the ligand showed a strong vibration band located at 1658 cm^{-1} which assigned to the carbonyl group ν(C=O) group of hydrazide moiety, whereas the weak and broad bands which observed at 3445, 3398, 3315, 3210 cm^{-1} assigned to the stretching vibration of the naphthanolic hydroxyl, aliphatic hydroxyl and ν(NH) groups associated through an intermolecular and intramolecular hydrogen bonding [27-31].These observations confirmed the presence of the ligand in the ketonic form in the solid state [29,31]. The spectrum of the ligand also showed bands at 1630 and 988 cm^{-1} which may be assigned to the azomethine groups ν(C=N) [32], and nitrogen-nitrogen linkages ν(N-N) respectively [33,34].

By comparing the IR spectral data of the complexes with that of the free ligand. It is noted that, in complexes (2),

**Table 1:** Electronic spectra and magnetic moments for ligand and its complexes.

No.	λ$_{max}$ (nm)	Transitions	Geometry	μ$_{eff}$ (BM)
(1)	265, 295, 315	π→π*, n→π*		-
(2)	265, 293, 305, 490, 565, 613	$^6A_{1g}$→^4E_g, $^6A_{1g}$→$^4T_{2g}$ and $^6A_{1g}$→$^4T_{1g}$	Octahedral	4.33
(3)	265, 285, 300, 485, 535, 600		Tetrahedral	2.80
(4)	256, 290, 303, 465, 622	$^4A_2$→$^4T_1$(F) (ν$_2$) and $^4A_2$→$^4T_1$(P) (ν$_3$)	Tetrahedral	2.11
(5)	256, 292, 305, 460, 518, 600	$^4T_{1g}$(F)→$^4T_{2g}$(P)(ν$_3$), $^4T_{1g}$(F)→$^4A_{2g}$(ν$_2$) $^4T_{1g}$(F)→$^4T_{2g}$(F)(ν$_1$)	Octahedral	2.82
(6)	265, 290, 302, 470, 630	$^4A_2$→$^4T_1$(F) (ν$_2$) and $^4A_2$→$^4T_1$(P) (ν$_3$)	Tetrahedral	5.26
(7)	265, 292, 305, 485, 605	$^3T_1$(F)→$^3A_2$ and $^3T_1$(F)→$^3T_1$(P)	Tetrahedral	2.32
(8)	265, 290, 306, 490, 530, 600, 835	O→Ni, $^3A_{2g}$(F)→$^3T_{1g}$(P) (ν$_3$), $^3A_{2g}$(F)→$^3T_{1g}$(F)(ν$_2$)	Distorted octahedral	2.40
(9)	256, 285, 300, 350, 475, 550, 630	O→Cu, $^2B_1$→^2E and $^2B_1$→$^2B_2$	Distorted tetragonal octahedral	1.58
(10)	265, 280, 300, 465, 530, 595			1.53
(11)	265, 286, 297, 420, 565	$^2T_2$(D)→^2E (D)	Tetrahedral	1.80
(12)	265, 285, 295, 420, 495, 590, 625	O→Cu, $^2B_1$→^2E and $^2B_1$→$^2B_2$	Distorted tetragonal octahedral	1.47
(13)	265, 290, 305, 424, 535, 595			1.61
(14)	265, 290, 310, 375			Diamagnetic
(15)	270, 290, 310, 370			
(16)	265, 292, 307, 365			
(17)	265, 290, 310, 360			
(18)	265, 285, 300, 360			
(19)	265, 290, 305, 365			

Table 2: ESR data for metal (II) complexes.

Complex	$g_\parallel$	$g_\perp$	$^a g_{iso}$	$A_\parallel$ (G)	$A_\perp$ (G)	$^b A_{iso}$ (G)	$^c G$	ΔE_{xy} (cm^{-1})	ΔE_{xz} (cm^{-1})	$K_\perp^2$	$K_\parallel^2$	K^2	K	$g_\parallel/A_\parallel$ (cm^{-1})	α^2	β^2	β_1^2	-2β	$a^2 d$ (%)
(2)	-	-	2.08	-	-	-	-	-	-	-	-	-	-	-	-	-	-	-	-
(9)	2.21	2.06	2.12	150	15	60	3.5	18182	21052	0.68	0.57	0.64	0.8	147	0.71	0.95	0.80	154.4	66
(10)	2.03	2.2	2.14	170	20	70	-	-	-	-	-	-	-	-	-	-	-	-	-
(11)	-	-	2.11	-	-	-	-	-	-	-	-	-	-	-	-	-	-	-	-
(12)	2.18	2.05	2.09	135	15G	55	3.6	16,949	20,202	0.58	0.45	0.535	0.73	167.7	0.6	0.96	0.75	146	62

$^a g_{iso} = (2g_\perp + g_\parallel)/3$, $^b A_{iso} = (2A_\perp + A_\parallel)/3$, $^C G = (g_\parallel - 2)/(g_\perp - 2)$. ESR=Electron spin resonance
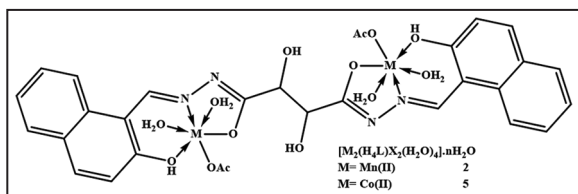
Figure 1: Suggested formulae of the Mn^{II} and Co^{II} complexes (2,5).
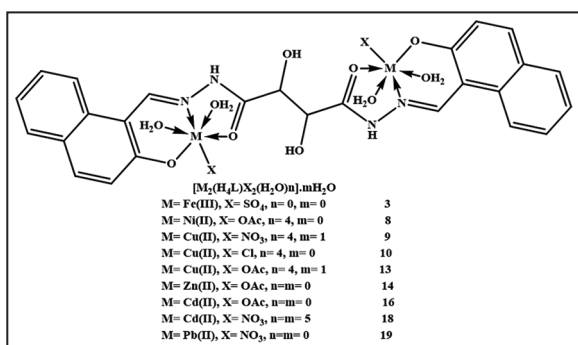
Figure 2: Suggested formulae of the Fe^{III}, Ni^{II}, Cu^{II}, Zn^{II}, Cd^{II} and Pb^{II} complexes (3, 10, 13, 14, 16, 18-19).
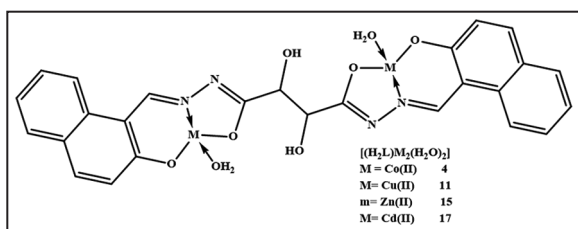
Figure 3: Suggested formulae of the Co^{II}, Cu^{II}, Zn^{II} and Cd^{II} complexes (4, 11, 15, 17).
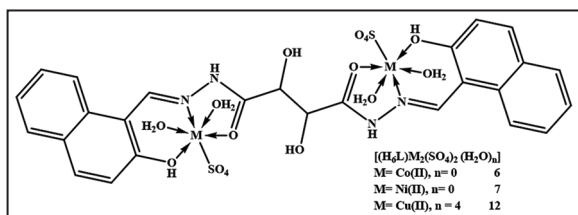
Figure 4: Suggested formulae of the Co^{II}, Ni^{II} and Cu^{II} complexes (6, 7, 12).

(4), (5), (11), (15) and (17) the bands characteristic to ν(NH) and ν(C=O) were disappeared. This may be due

to the bonding of the ligand to the metal ions in the enolic form, via the enolic carbonyl oxygen atoms. This result is also supported by the appearance of a new band in the ranges of 1603-1581 cm^{-1} which may be assigned to the C=N-N=C group [31]. In the spectra of all complexes except (2), (4), (5), (11), (15) and (17) the absorption frequency of amide carbonyl groups ν(C=O) was shifted to lower frequency side about 7-39 cm^{-1} and appeared in the region 1619-1658 cm^{-1} with lowering its intensity confirmed the coordination of oxygen atom of amide ν(C=O) with the metal ions without undergoing enolization. In the IR spectra of complexes (3), (4), (8-11), and (13-19), it was observed that the absence of absorption band due to naphthanolic hydroxyl group which appeared in the spectrum of ligand at 3446 indicated to the formation of bond between metal ion and naphthanolic hydroxyl oxygen atom via deprotonation. This is further confirmed by the increase in absorption frequency about 19-41 cm^{-1} of phenolic ν(C-O) which appeared in the region 1284-1331 cm^{-1} indicating the participation of the oxygen atom of naphthanolic hydroxyl group in bonding to metal ions [35].[31] In the spectra of all complexes the absorption frequency of azomethine ν(C=N) function shifted to lower frequency side about 7-26 cm^{-1} with decreasing their intensities and appeared in the region 1604-1623 cm^{-1} suggesting the involvement of nitrogen atom of azomethine function in complexation with the metal ions [35]. At the same time, the characteristic band of the ν(N–N) which appeared in the spectra of the ligand at 988 cm^{-1} is shifted to lower frequency and appeared in the 989-1030 cm^{-1} in the spectra of metal complexes. These negative shifts of ν(C=N) and positive shifts of ν(N–N) bands confirmed that the azomethine nitrogen atoms participated in coordination with the metal ions [36]. The appearance of new bands appeared in the ranges 530-684, 510-581 and 456-533 cm^{-1} for different complexes may be assigned to the ν(M–O), (M←O) and ν(M←N), respectively, [30,37]. These results confirmed that the bonding of the ligand with the metal occurred via enolic carbonyl oxygen, azomethine nitrogen and naphthanolic hydroxyl oxygen atoms. In acetate complexes, the acetate ion may be coordinate to the metal ion in unidentate, bidentate, or bridging bidentate manner. The ν_{as}(CO$_2$)

Table 3: Thermal analyses for metal (II) complexes.

Compound no. molecular formula	Temperature (°C)	DTA (peak)		TGA (Wt. loss %)		Assignments
		Endo	Exo	Calcd.	Found	
Complex (2) $[(H_4L)(Mn)_2(OAc)_2(H_2O)_4].H_2O$	45	Endo	-	-	-	Broken of H-bonding
	65	Endo	-	2.24	2.00	Loss of (H_2O) hydrated water molecules
	165	Endo	-	8.96	8.66	Loss of coordinated $4H_2O$ molecule
	250	Endo	-	14.78	15.03	Loss of coordinated two acetate groups
	350	Endo	-	-	-	Melting point
	370, 410, 435, 500		Exo	64.14	64.76	Decomposition process with the formation of MnO
Complex (6) $[(H_6L) Co_2(SO_4)_2]$	50	Endo	-	-	-	Broken of H-bonding
	250	Endo	-	24.05	24.9	Loss of coordinated two SO_4 group
	340	Endo	-	-	-	Melting point
	405, 450, 485, 510, 530	-	Exo	65.32	66.57	Decomposition process with the formation of CoO
Complex (9) $[(H_4L) Cu)(NO_3)_2(H_2O)_4]$	50	Endo	-	-	-	Broken of H-bonding
	160	Endo	-	8.90	8.63	Loss of $(4H_2O)$ coordinated water molecules
	250	Endo	-	14.65	15.32	Loss of coordinated two NO_3 group
	360	Endo	-	-	-	Melting point
	350, 380, 450, 500, 610	-	Exo	65.94	65.11	Decomposition process with the formation of CuO
Complex (10) $[(H_4L)(Cu)_2Cl_2(H_2O)_4]$	50	Endo	-	-	-	Broken of H-bonding
	140	Endo	-	9.55	10.10	Loss of $(4H_2O)$ coordinated water molecules
	230	Endo	-	9.40	9.21	Loss of coordinated two chloride ions
	330	Endo	-	-	-	Melting point
	370, 390, 420, 450, 500	-	Exo	70.51	68.94	Decomposition process with the formation of CuO
Complex (13) $[(H_4L)(Cu)_2(OAc)_2(H_2O)_4].H_2O$	45	Endo	-	-	-	Broken of H-bonding
	60	Endo	-	2.2	1.97	Loss of (H_2O) hydrated water molecules
	130			8.79	9.12	Loss of coordinated four water molecules
	190	Endo	-	14.5	14.01	Loss of coordinated two acetate groups
	340	Endo	-	-	-	Melting point
	365, 450, 550, 600	-	Exo	64.80	62.62	Decomposition process with the formation of CuO
Complex (16) $[(H_4L)(Cd)_2(OAc)_2]$	50	Endo	-	-	-	Broken of H-bonding
	210	Endo	-	14.33	13.78	Loss of coordinated two acetate groups
	345	Endo	-	-	-	Melting point
	370, 390, 410, 450, 510	-	Exo	70.18	68.11	Decomposition process with the formation of CdO
Complex (19) $[(H_4L)(Pb)_2(NO_3)_2]$	60	Endo	-	-	-	Broken of H-bondings
	240	Endo	-	11.60	12	Loss of coordinated two NO_3 groups
	320	Endo	-	-	-	Melting point
	460		Exo	54.52	52.23	Decomposition process with the formation of PbO

TGA=Thermal gravim analysis, DTA=Differential thermal analysis

and $v_s(CO_2)$ of the free acetate ion are Ca 1560 and 1416 cm^{-1} respectively. In unidentate acetate complexes $v(C=O)$ is higher than $v_s(CO_2)$ and $v(C-O)$ is lower than $v_{as}(CO^{2-})$. As a result, the separation between the two $v(CO)$ is much larger in unidentate than in free ion but in bidentate the separation is lower than in the free ion while in bridging bidentate the two $v(CO)$ is closer to the free ion [38]. In the case of acetate complexes (2), (5) (8), (13), (14) and (16) there are two new bands appeared in the 1555-1570 and 1337-1399 cm^{-1} ranges which are attributed to the symmetric and asymmetric stretching vibration of the acetate group. The mode of coordination of acetate group has often been deduced from the magnitude of the observed separation between the $v_{asy.}(COO^-)$ and $v_{sy.}(COO^-)$. The separation values (Δ) between $v_{asym}(COO^-)$ and $v_{sym.}(COO^-)$ in these complexes were in the 167-221 cm^{-1} range suggesting the coordination of acetate group in as a monodentate fashion [39,40]. The IR spectra of the nitrate complexes (9), (18) and (19) showed bands in the v_5(1433-1459), v_1(1359-1383) and v_2(870-880) ranges indicating the nitrate group coordinated to the metal ion. The differences between the two high bands (v_5-v_1) are in the 74-78 cm^{-1} indicating that, the nitrate ion bonded to the copper(II) ion is unidentate manner [38,40,41]. In the case of sulfate complexes (3), (6), (7), (12) and (15) there are new bands appeared in the 1184-1194, 1118-1141, 830-870 ranges for the complexes, respectively. These bands indicate that the sulfate ion is coordinated to the metal ion as chelating unidentate fashion [38,42].

The above results together with elemental analysis indicates that the ligand behaved as neutral, monobasic or dibasic hexadentate ligand bonded to the metal ions through enolic or ketonic carbonyl oxygen atoms, azomethine and protonated or deprotonated naphthanolic hydoxyl oxygen atoms.

3.3 ^{1}*H-NMR Spectra of the Ligand (1) and Cd^{II} Complex (16)*

The ^{1}H-NMR spectrum of the ligand (H$_6$L) shows the absence of the signal of the amino group (NH$_2$) characteristic of the starting material (hydrazide). The spectrum shows three sets of peaks; the first one observed as a singlet at 12.90 (*s*, 2H[14,36]), 9.98 (*s*, 2H[13,23]) 9.67 (*s*, 2H[18,19]) ppm which may be assigned naphthanolic hydroxyl protons, azomethine protons and aliphatic hydroxyl protons respectively. These hydrogen resonances appear at high δ values because of their attachment to highly electronegative atoms, oxygen and nitrogen, respectively; hence, they are in a low electron density environment. This assignment was confirmed by the deuterated spectra in which the intensity of these bands was considerably decreased. The position of these peaks in the downfield region indicates the possibility of extensive

hydrogen bonding involving these groups [40]. The second set appeared as a singlet at 8.88 (*s*, 2H[11,25]), ppm and corresponded to the azomethine proton (H–C=N) [36]. The third group appeared as multiplets in the 7.15-8.11 (m, 12 H) ppm range, which were attributed to aromatic protons. The signal appeared at 4.67 ppm may be assigned to (HO-C*H*[16,17]). It is clear from the ^{1}H-NMR spectrum of the ligand that it exists in the keto form only with no evidence for the presence of the enol form [42,43]. This result was confirmed by the appearance of the signal of the azomethine (NH), naphthanolic and aliphatic (OH) only and the absence of the (OH) signal of the enolic form. The same conclusion was reported by many authors [24,36]. Comparing the ^{1}H-NMR spectra of the cadmium^{II} complexes, 16, with that of the free ligand, it could be noticed that the signals of the naphthanolic OH groups had disappeared, indicating that the ligand bonded to the cadmium ions as a dibasic ligand *via* the deprotonated hydroxyl oxygen atoms while the protons of azomethine were still present. A significant downfield shift of the azomethine proton signal in the complexes relative to the corresponding signal of the free ligand confirmed the coordination of the azomethine nitrogen atom to the metal [43,44].

3.4. Mass Spectra of the Ligand

The mass spectrum of the ligand supports the suggested structure of the ligand. It reveals molecular ion peak m/z at 486 is consistent with the molecular weight of the ligand. Moreover, the ligand splits to several fragments which possessed ion peaks equal to m/z=429, 404, 300, 186, 169, 115, and 89 which corresponding to $C_{16}H_{21}N_4O_{10}$, $C_{14}H_{20}N_4O_{10}$, $C_{11}H_{14}N_3O_7$, $C_7H_{12}N_3O_3$, $C_6H_7N_3O_3$, $C_4H_7N_2O_2$ and$C_2H_7N_2O_2$, respectively.

3.5. Magnetic Moments

The magnetic moments of the metal complexes (2)-(19) at room temperatures are shown in Table 1. Mn^{II} complex (2) and Fe^{III} complex (3) show magnetic moment values equal 4.33 and 2.8 B.M, respectively. These values are lower than expected to high spin manganese(II) and iron(III) configuration (d^5). This phenomenon may be due to antiferromagnetic spin-spin interaction between metal(II) ions through molecular association or hydrogen bonding [45]. Co^{II} complex (**4-6**) show magnetic moment value in the 2.11-2.82 B.M, which are lower than expected to high spin cobalt(II). This lowering in the magnetic value may be due to antiferromagnetic spin-spin interaction between cobalt(II) ions through molecular association. Ni^{II} complexes (7-8) show values equal to 2.32 and 2.40 B.M range. The lowering in these values may be assigned to the interaction between the two nickel atom via hydrogen bonding or molecular association [43,45]. Cu^{II} complexes (9-13) show values in the 1.47-1.61 B.M, range corresponding to one unpaired electron. The low values of complexes

are due to spin-spin interactions take place through hydrogen bonding [43,45]. Zinc(II) complexes (14) and (15), cadmium(II) complexes (16-18) and lead(II) complex (19) show diamagnetic property.

3.6. Electronic Spectra

The electronic spectral data for the ligand (1) and its metal complexes in nujol mull are summarized in Table 1. The electronic absorption spectra of the ligand showed that it exhibited three bands located at 265, 295 and 315 nm. The first one assigned to intraligand $\pi \rightarrow \pi^*$ transition in the napthanolic moiety which is nearly unchanged on complexation. The second and third bands may be assigned to $n \rightarrow \pi^*$ and charge transfer transition of the azomethine and carbonyl groups. The location of these bands was found to be shifted to higher energy on complexation. This finding indicated to the participation of these groups in bonding and coordination with metal ions [28,46]. In addition, the spectra of the complexes were showed new bands laid in the range 360-375 nm which may be attributed to the charge-transfer bands [47]. Manganese(II) complex (2) show bands at 490, 565 and 613 nm, corresponding to $^6A_{1g} \rightarrow ^4E_g$, $^6A_{1g} \rightarrow ^4T_{2g}$ and $^6A_{1g} \rightarrow ^4T_{1g}$ transitions which are compatible to an octahedral geometry around the Mn(II) ions [46,48]. Iron(III) complex (3) shows bands at 485, 535 and 670 nm, are due to charge transfer and $^6A_1 \rightarrow ^4A_1(v2)$ and $^6A_1 \rightarrow ^4T_2(v3)$, transitions, suggesting the tetrahedral geometry around the iron(III) ion [46,49]. Cobalt(II) complexes (4) and (6) show bands at 465, 470 and 622, 630 nm, respectively, these bands are assigned to $^4A_2 \rightarrow ^4T_1(F)$ (v_2) and $^4A_2 \rightarrow ^4T_1(P)$ (v_3), transitions, respectively, assuming tetrahedral geometry around the Co(II) ion [46,50]. However, cobalt(II) complex (5) show bands at 460, 518, and 600 nm, these bands are assigned to $^4T_{1g}(F) \rightarrow ^4T_{2g}(P)$ (v_3), $^4T_{1g}(F) \rightarrow ^4A_{2g}(v_2)$ and $^4T_{1g}(F) \rightarrow ^4T_{2g}(F)(v_1)$ transitions respectively [46,51]. The electronic spectrum nickel(II) complexes (7) shows bands at 485 and 605 nm, which are assignable to $^3T_1(F) \rightarrow ^3A_2$ and $^3T_1(F) \rightarrow ^3T_1(P)$, respectively, assuming the tetrahedral geometry around the Ni(II) ions [46,50]. However, nickel(II) complex (8) shows bands in the 490, 530, 600, and 835 nm ranges, the first band is attributable to O→Ni charge transfer, while the other three bands are assigned to $^3A_{2g}(F) \rightarrow ^3T_{1g}(P)$ (v_3), $^3A_{2g}(F) \rightarrow ^3T_{1g}(F)(v_2)$ and $^3A_{2g}(F) \rightarrow ^3T_{2g}(F)(v_1)$ transitions, respectively, indicating an octahedral Ni(II) geometry [46,52].

The v_2/v_1 ratio for the complex is 1.39 which are less than the usual range of 1.5-1.75, indicating a distorted octahedral Ni(II) complex [53]. Copper(II) complexes (9-10) and (12-13) show bands in the 490-465, 580-540 and 615-600 nm ranges, are assigned to O→Cu, charge transfer, $^2B^1 \rightarrow ^2E$ and $^2B_1 \rightarrow ^2B_2$ transitions, indicating a distorted tetragonal

octahedral structure [54,55]. However, copper(II) complexes (11) exhibited one band at 565 nm that is assigned to $^2T_2(D) \rightarrow ^2E(D)$ transition, indicating that, this complex has a tetrahedral geometry [32,56]. The possibility of square planar geometry at metal center was ruled out because in general square-planar complexes are known to exhibit two band in the visible region, around 700-712 nm and 533-550 nm reported by El-Tabl *et al.* [57] was not observed in the case of our synthesized complex. Zinc complexes (14) and (15), cadmium(II) complexes (16-18) and lead(II) complex (19) show bands due to intraligand transitions.

3.7. ESR

The ESR spectral data for complexes (2) and (9-12) are presented in Table 2. The ESR spectra of manganese(II) and copper(II) complexes (2) and (11) at room temperature give one broad isotropic signal with g_{iso} values at 2.08 and 2.11 for the two complexes, respectively [42,58]. The ESR spectra of copper(II) complexes (9) and (12) at room temperature are characteristic of species d^9 configuration having axial type of a $d_{(x2-y2)}$ ground state which is the most common for copper(II) complexes [59,60]. These complexes show $g_{\parallel} > g_{\perp} > 2.0023$, indicating octahedral geometry around copper(II) ion [61,62]. The g-values are related by the expression $G = (g_{\parallel}-2)/(g_{\perp}-2)$ [61,63], where, (G) exchange coupling interaction parameter (G). If $G < 4.0$, a significant exchange coupling is present, whereas if G value > 4.0, local tetragonal axes are aligned parallel or only slightly misaligned. Complexes (9) and (12) show 3.5 and 3.6 values indicating spin-exchange interactions take place between copper(II) ions. This phenomena is further confirmed by the magnetic moments values (1.58 and 1.47 BM). The $g_{\parallel}/A_{\parallel}$ value is also considered as a diagnostic term for stereochemistry [64], the $g_{\parallel}/A_{\parallel}$ values in the $(105-135 \text{ cm}^{-1})$ range are expected for copper complexes within perfectly square planar geometry and for tetragonal distorted octahedral complexes are 150-250 cm^{-1}. The $g_{\parallel}/A_{\parallel}$ values for the copper complexes (9) and (12) are 147 and 167.7 cm^{-1} which lie just within the range expected for the tetragonal distorted octahedral copper(II) complexes (Table 2). The g-value of the copper (II) complexes with a $^2B_{1g}$ ground state $(g_{\parallel} > g_{\perp})$ may be expressed by the following equations [65]:

$$g_{\parallel} = 2.002 - (8K^2_{\parallel} \lambda°/\Delta E_{xy}) \qquad (1)$$

$$g_{\perp} = 2.002 - (2K^2_{\perp} \lambda°/\Delta E_{xz}) \qquad (2)$$

Where, $k_{\parallel}$ and $k_{\perp}$ are the parallel and perpendicular components respectively of the orbital reduction factor (K), $\lambda°$ is the spin-orbit coupling constant for the free copper, ΔE_{xy} and ΔE_{xz} are the electron transition energies of $^2B_{1g} \rightarrow ^2B_{2g}$ and $^2B_{1g} \rightarrow ^2E_g$. From the above relations, the orbital reduction factors $(K_{\parallel}, K_{\perp}, K)$,

which are measure terms for covalency [66], can be calculated. For an ionic environment, K=1; while for a covalent environment, K<1. The lower the value of K, the greater is the covalency.

$$K^2_\perp = (g_\perp - 2.002) \, \Delta E_{xz}/2\lambda_o \qquad (3)$$

$$K^2_\parallel = (g_\parallel - 2.002) \, \Delta E_{xy}/8\lambda_o \qquad (4)$$

$$K^2 = (K_{2\parallel} + 2K^2_\perp)/3 \qquad (5)$$

K values (Table 2), for the copper(II) complexes (9) and (12) are indicating for a covalent bond character [60,67].[42,70] Kivelson and Neiman noted that, for ionic environment $g_\parallel \geq 2.3$ and for a covalent environment $g_\parallel < 2.3$ [68]. Theoretical work by Smith [66] seems to confirm this view. The g-values reported here (Table 2) show considerable covalent bond character [69]. Furthermore, the in-plane σ-covalency parameter, α^2(Cu) was calculated by:

$$\alpha^2 \, (Cu) = (A_\parallel/0.036) + (g_\parallel - 2.002) + 3/7(g - 2.002) + 0.04 \qquad (6)$$

The calculated values (Table 2) suggest a covalent bonding [40,43,57,59]. The in-plane and out of-plane π-bonding coefficients β^2_1 and β^2, respectively, are dependent on the values of ΔE_{xy} and ΔE_{xz} in the following equations [61].

$$\alpha^2\beta^2 = (g_\perp - 2.002) \, \Delta E_{xy}/2\lambda_o \qquad (7)$$

$$\alpha^2\beta^2_1 = (g_\parallel - 2.002) \, \Delta E_{xz}/8\lambda_o \qquad (8)$$

In this work, the complexes (9) and (12) show β^2_1 values 0.80 and 0.75 indicating a moderate degree of covalency in the in-plane π-bonding [67,70] β^2 value forcomplexes (9) and (4) equal 0.95 and 0.96 indicating a covalent bonding character out-of- plane π-bonding [67,70]. It is possible to calculate approximate orbital populations for d-orbitals by [71]:

$$A_\parallel = A_{iso} - 2B[1 \pm (7/4) \, \Delta g_\parallel] \quad \Delta g_\parallel = g_\parallel - g_e \qquad (9)$$

$$\alpha^2_{p,d} = 2B/2B° \qquad (10)$$

Where, A° and 2B° is the calculated dipolar coupling for unit occupancy of d orbital respectively. When the data are analyzed, the components of the [63]Cu hyperfine coupling were considered with all the sign combinations. The only physically meaningful results are found when $A_\parallel$ and $A_\perp$ were negative. The resulting isotropic coupling constant was negative, and the parallel component of the dipolar coupling 2B are negative (−154.4 and −146 G). These results can only occur for an orbital involving the d_{x2-y2} atomic orbital on copper. The value for 2B is quite normal for copper(II) complexes [71]. The |A_{iso}| value was

relatively small. The 2B value divided by 2B° (The calculated dipolar coupling for unit occupancy of d_{x2-y2} (−235.11 G), using Equation (10) suggests all orbital population are 66 and 62% d-orbital spin density, clearly the orbital of the unpaired electron is d_{x2-y2} [69]. The ESR spectrum of copper(II) complex (10) at room temperature is interesting to note that $g_\perp$ is greater than $g_\parallel$, indicating a compressed tetragonal distortion along the Z-axis [72,73]. This distortion lowers the energy of $d_{(x2-y2)}$, and hence it is one of the very few tetragonal complexes with the unpaired electron in the d_{z2} orbital [72,73]. The compression along the Z-axis results in an increased bond length in the X-Y plane. The g-values are $g_\parallel = 2.03$ with $A_\parallel = 170$ G and $g_\perp = 2.20$ with $A_\perp = 20$ G respectively [72,73].

3.8. Thermal Analyses (DTA and TGA)

Since the IR spectral data indicates the presence of water molecules, thermal analyses (DTA and TGA) were carried out to certain their nature. The thermal curves in the temperature 27-600° range for complexes (2), (3), (9), (10), (13), (16), and (19) are thermally stable up to 45°C. Broken of hydrogen bonding occurs as an endothermic peak within the temperature 45-50°C as shown in Table 3. Dehydration is characterized by endothermic peaks within the temperature 60-65°C range, corresponding to the loss of hydrated water molecules as in complexes (2) and (13). The elimination of coordinated water molecules occur in 130-165°C range accompanied by endothermic peaks as in complexes (2), (10) and (13) [74,75]. The TGA and DTA thermogram of manganese(II) complex (2) showed that this complex decomposed in six step. The first occurred at 45°C with no weight loss as endothermic peak, may be due to break of hydrogen bonding. The second step occur at 65°C with 2.00% weight loss (Calcd. 2.24%) as endothermic peak which could be due to the elimination of one hydrated water molecules. The third step occurred at 165°C with 8.66% weight loss (Calcd. 8.96%) could be due to the elimination of four coordinated water molecules. The fourth decomposition step which occurred at 250°C with 15.03% weight loss (Calcd. 14.78%), could be attributed to the loss of coordinated two acetate groups. The complex shows an exothermic peak observed at 350°C is due its melting point. Finally, exothermic peaks appear at 370, 410, 435 and 500°C corresponding to oxidative thermal decomposition which proceeds slowly with leaving MnO with 64.76% weight loss (Calcd. 64.14%) [76]. The TGA and DTA thermogram of cobalt(II) Complex (6) show endothermic peak occurred at 50°C with no weight loss as endothermic peak, may be due to break of hydrogen bonding. While the endothermic peak that, observed at 250°C with 24.05% weight loss (Cacld. 24.90%) are assigned the elimination of two sulfate ions. Another exothermic peak observed at 340 with no weight loss may be due to its melting point.

Finally, the complex shows exothermic peaks at 405, 450, 485, 510 and 530°C with 65.32% weight loss (Cacld. 66.57%) corresponding to oxidative thermal decomposition which proceeds slowly with final residue CoO [76]. The TGA and DTA thermogram of copper(II) complex (9) shows endothermic peak at 50°C which assigned to the breaking of hydrogen bonding. Another endothermic peak was showed at 160°C, with 8.60% weight loss (Cacld. 8.9%), due to loss of four coordinated water molecules. While the endothermic peak which was showed at 250°C with weight loss 14.65 (Cacld. 15.32%), may be attributed to the elimination of two nitrate ions. The complex displayed another exothermic peak at 360°C may be assigned to its melting point. Oxidative thermal decomposition occurs in the 350, 380, 450, 500 and 610°C with exothermic peaks, leaving CuO with 65.11% weight loss (Cacld. 65.94%) [76]. The TGA and DTA thermogram of copper(II) complex (10) shows an endothermic peak at 50°C due to break of hydrogen bonding and another endothermic peak at 140°C with 10.10% weight loss (Cacld. 9.55%) is assigned to the loss of four coordinated water molecules. While the endothermic peak at 230°C with 9.21% weight loss (Cacld. 9.4%) is due to loss of two chloride ions. The endothermic peak which appeared 330 could be due to melting point. Oxidative thermal decomposition occurs at 370, 390, 420, 450 and 500°C with exothermic peaks, leaving CuO with 68.94% weight loss (Cacld. 70.51%) [76]. The TG and DTA thermogram of copper(II) complex (13) shows an endothermic peak at 45°C due to break of hydrogen bonding and another endothermic beak at 60°C, with 1.97% weight loss (Cacld. 2.20 %) due to loss of one hydrated water molecule. The endothermic peak observed at 130°C with 9.12% weight loss (Cacld. 8.80%), is assigned to loss of four coordinated water molecules. The endothermic peak observed at 190°C with 14.01% weight loss (Cacld. 14.50%) is due to the elimination of coordinated acetate groups. Another exothermic peak observed at 340°C may be assigned to its melting point. Oxidative thermal decomposition occurs at 365, 450, 550 and 600°C with exothermic peaks, leaving CuO with 62.62% weight loss (Cacld. 64.80%) [76].

The thermal analysis curve of cadmium(II) complex (16) decomposed in four steps. The first peak was observed as an endothermic peak at 50°C due to break of hydrogen bonding while the second endothermic peak observed at 210°C with 13.78% weight loss (Cacld. 14.33%) is due to the elimination of coordinated acetate groups. Another exothermic peak observed at 345°C may be assigned to its melting point. Oxidative thermal decomposition occurs at 370, 390, 410, 450 and 510°C with exothermic peaks, leaving CdO with 68.11% weight loss (Cacld. 70.18%) [76]. The thermal analysis curve of lead(II)

complex (19) decomposed in four steps. The first beak was observed as an endothermic peak at 60°C due to break of hydrogen bonding while the second endothermic peak observed at 240°C with 13.78% weight loss (Cacld. 14.33%) is due to the elimination of coordinated nitrate groups. Another exothermic peak observed at 320°C may be assigned to its melting point. Oxidative thermal decomposition occurs at 460°C with exothermic peaks, leaving PbO with 52.23% weight loss (Cacld. 54.52%) [76].

3.9. Chemotherapeutic Studies

The cytotoxicity activity of the ligand (1) and its metal complexes (2), (4), (9), (10), (12), (13), and (18) were evaluated against either HEPG-2 cell line or MCF-7 cell line and shown in Figures 5 and 6. In this study, we try to know the chemotherapeutic activity of the tested complexes by comparing them with the standard drug (IMURAN (azathioprine)). The treatment of the different complexes in DMSO showed similar effect in the tumoral cell line used as it was previously reported [77]. The solvent DMSO shows no effect in cell growth. The ligand (1) shows a weak inhibition effect at ranges of concentrations used, however, the complexes showed a better effect against HEPG-2 and MCF-7 cell lines. The obtained data indicate the surviving fraction ratio against HEPG-2 tumor and MCF-7 cell lines increasing with the decrease of the concentration in the range of the tested concentrations. Cytotoxicity results indicated that the tested Fe(II) complex (2) and Cu(II) (12) (IC$_{50}$ =0.91, 5.12 µg ml^{-1}, respectively) demonstrated potent cytotoxicity against MCF-7 cancer cells while Cd(II) complex (18) demonstrated the most potent cytotoxicity against HepG2 cancer cells with IC$_{50}$ = 3.7 (Figure 6). The chemotherapeutic activity of the complexes may be attributed to the central metal atom which was explained by Tweedy's chelation theory [77,78]. Also, the positive charge of the metal increases the acidity of coordinated ligand that bears protons, leading to stronger hydrogen bonds which enhance the biological activity [79,80]. Moreover, Gaetke and Chow had reported that metal has been suggested to facilitate oxidated tissue injury through a free-radical mediated pathway analogous to the Fenton reaction [80]. By applying the ESR-trapping technique, evidence for metal - mediated hydroxyl radical formation *in vivo* has been obtained [64]. Reactive oxygen species are produced through a Fenton-type reaction as follows:

$$LM(II) + H_2O_2 \rightarrow LM(I) + .OOH + H+$$

$$LM(I) + H_2O_2 \rightarrow LM(II) + .OH + OH-$$

Where L, organic ligand

Furthermore, metal could act as a double-edged sword by inducing DNA damage and also by inhibiting their repair [81]. The OH radicals react with DNA sugars and
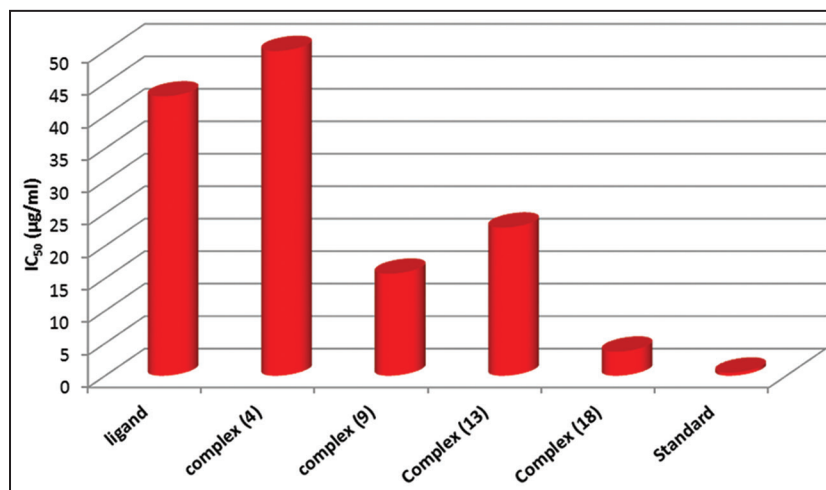
Figure 5: Inhibitory concentration 50% values of the ligand, H_2L (1) and its metal complexes against human hepatic HEPG-2 cell line.
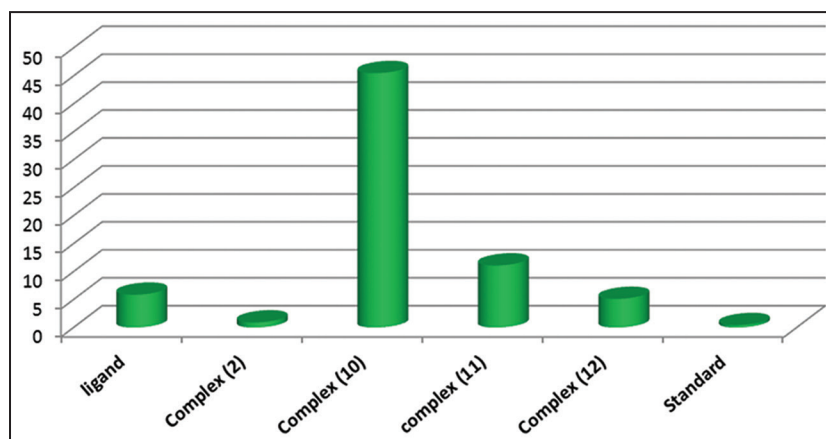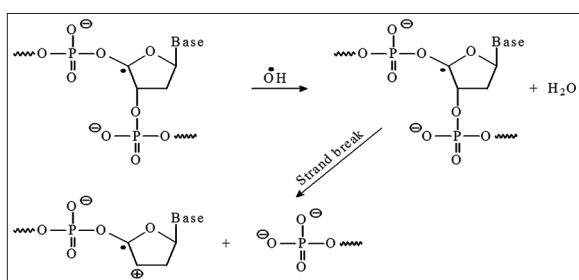

Figure 6: Inhibitory concentration 50% values of the ligand, H_2L (1) and its metal complexes against breast cancer MFC-7 cell line.

Scheme 2: Proposed mechanism of DNA damage. OH radicals react with DNA sugars and bases, resulting in the release of free bases and strand break occurs.

bases and the most significant and well-characterized of the OH reactions is hydrogen atom abstraction from the C4 on the deoxyribose unit to yield sugar radicals with subsequent β-elimination (Scheme 2). By this mechanism strand break occurs as well as the release of the free bases. Another form of attack on the DNA bases is by solvated electrons, probably via a similar reaction to those discussed below for the direct effects of radiation on DNA [66].

4. CONCLUSION

Noval Schiff base ligand, 1,2-bis(phenylamino)vinyl) hydrazono)methyl)phenol and its copper(II), Nickel(I), cobalt(II), manganese(II), zinc(II), cadmium(II), lead(II), stronchium(II), thalous(I) and iron(II) metal complexes were synthesized. The analytical and physicochemical data confirmed the composition and structure of the newly obtained compounds. The ESR spectra of solid Cu(II) complexes (2-5) show axial type indicating a $d_{(x^2-y^2)}$ or $d_{(z^2)}$ ground state with significant covalent bond character. The ligand behaved as monobasic or neutral bidentate. The complexes adopted distorted octahedral geometry around the metal ion. The ligand recorded weak cytotoxic activity in the time that some complexes were very prospective compared to ALMURAN (zathiopeine) standard drug. This indicates enhancing of antitumor activity upon the coordination process. Fe(II) complex (2) showed the highest cytotoxic activity against MCF-7 with IC_{50} 0.91 µg ml^{-1}. This finding indicated to a very promising candidate as anti-breast carcinoma meanwhile, Cd(II) complex (18) recorded the highest activity against Hep-G2 (human liver cancer) with IC_{50} 3.7 µg ml^{-1}.

125

5. REFERENCES

1. G. Matelaa, R. Amana, C. Sharmab, S. Chaudharyc, (2013) Synthesis, characterization and antimicrobial evaluation of diorganotin (IV) complexes of schiff base, *Indian Journal of Advances in Chemical Science,* **1:** 157-163.

2. S. V. Babu, K. H. Reddy, (2013) Second derivative spectrophotometric determination of copper (II) using 2-acetylpyridine semicarbazone in biological, leafy vegetable and synthetic alloy samples, *Indian Journal of Advances in Chemical Science,* **1:** 105-111.

3. I. Correia, P. Adão, S. Roy, M. Wahba, C. Matos, M. R. Maurya, F. Marques, F. R. Pavan, C. Q. F. Leite, F. Avecilla, (2014) Hydroxyquinoline derived vanadium(IV and V) and copper(II) complexes as potential anti-tuberculosis and anti-tumor agents, *Journal of Inorganic Biochemistry,* **41:** 83-93.

4. S. Kondaiah, G. N. R. Reddy, D. Rajesh, J. Joseph, (2013) Synthesis, characterization, and antibacterial activity of the schiff base derived from P-toluic hydrazide and O-vanilin (OVPTH Ligand) and its Mn (II), Co (II), Ni (II) and Cu (II) complexes, *Indian Journal of Advances in Chemical Science,* **1:** 228-235.

5. A. S. El-Tabla, M. M. E. Shakdofa, M. A. Whaba, (2015) Synthesis, characterization and fungicidal activity of binary and ternary metal(II) complexes derived from 4,4′-((4-nitro-1,2-phenylene) bis(azanylylidene))bis(3-(hydroxyimino) pentan-2-one), *Spectrochimica Acta Part A: Molecular and Biomolecular Spectroscopy,* **136:** 1941-1949.

6. R. M. El-Bahnasawy, F. A. El-Saied, E. H. A. Gaafer, M. A. Wahba, (2013) Benzil bisisonicotinoyl hydrazone complexes of tervalent metals Ti, Zr, Sn, Hf and Th, *Inorganic Chemistry: An Indian Journal,* **8:** 1-6.

7. A. El-Tabl, M. A. E. Wahed, M. A. Wahba, (2015) Spectroscopic characterization and cytotoxic activity of new metal complexes derived from (1E, N'Z, N'Z)-N',N'-bis(2-hydroxybenzylidene)-2-(naphthalen-1-yloxy) acetohydrazonohydrazide, *Journal of Advances in Chemistry,* **11:** 3888-3918.

8. A. S. El-Tabl, M. M. A. E. Wahed, M. A. Wahba, S. A. El-assaly, L. M. Saad, (2014) sugar hydrazone complexes; Synthesis, spectroscopic characterization and antitumor activity, *Journal of Advances in Chemistry,* **9:** 1837-1860.

9. A. Bacchi, M. Carcelli, P. Pelagatti, G. Pelizzi, M. Rodriguez-Arguelles, D. Rogolino, C. Solinas, D. F. Zani, (2005) Antimicrobial and mutagenic properties of organotin (IV) complexes with isatin and N-alkylisatin bisthiocarbonohydrazones, *Journal of Inorganic Biochemistry,* **99:** 397-408.

10. A. Para, S. Karolczyk-Kostuch, M. Fiedorowicz, (2004) Dihydrazone of dialdehyde starch and its metal complexes, *Carbohydrate Polymers,* **56:** 187-193.

11. A. Bacchi, A. Bonardi, M. Carcelli, P. Mazza, P. Pelagatti, C. Pelizzi, G. Pelizzi, C. Solinas, F. Zani, (1998) Organotin complexes with pyrrole-2, 5-dicarboxaldehyde bis (acylhydrazones). Synthesis, structure, antimicrobial activity and genotoxicity, *Journal of Inorganic Biochemistry,* **69:** 101-112.

12. A. El-Asmy, O. El-Gammal, H. Radwan, (2010) Synthesis, characterization and biological study on Cr 3+, ZrO 2+, HfO 2+ and UO 2 2+ complexes of oxalohydrazide and bis (3-hydroxyimino) butan-2-ylidene)-oxalohydrazide, *Spectrochimica Acta Part A: Molecular and Biomolecular Spectroscopy,* **76:** 496-501.

13. A. A. El-Asmy, O. El-Gammal, H. Radwan, S. Ghazy, (2010) Ligational, analytical and biological applications on oxalyl bis (3, 4-dihydroxybenzylidene) hydrazone, *Spectrochimica Acta Part A: Molecular and Biomolecular Spectroscopy,* **77:** 297-303.

14. H. Hosseini-Monfared, N. Asghari-Lalami, A. Pazio, K. Wozniak, C. Janiak, (2013) Dinuclear vanadium, copper, manganese and titanium complexes containing O, O, N-dichelating ligands: Synthesis, crystal structure and catalytic activity, *Inorganica chimica acta,* **406:** 241-250.

15. S. S. Machakanur, B. R. Patil, D. S. Badiger, R. P. Bakale, K. B. Gudasi, S. W. Annie Bligh, (2012) Synthesis, characterization and anticancer evaluation of novel tri-arm star shaped 1,3,5-triazine hydrazones, *Journal of Molecular Structure,* **1011:** 121-127.

16. A. A. El-Asmy, A. Al-Abdeen, W. A. El-Maaty, M. Mostafa, (2010) Synthesis and spectroscopic studies of 2, 5-hexanedione bis (isonicotinylhydrazone) and its first raw transition metal complexes, *Spectrochimica Acta Part A: Molecular and Biomolecular Spectroscopy,* **75:** 1516-1522.

17. O. B. Chanu, A. Kumar, A. Ahmed, R. Lal, (2012) Synthesis and characterisation of heterometallic trinuclear copper (II) and zinc (II) complexes derived from bis (2-hydroxy-1-naphthaldehyde) oxaloyldihydrazone, *Journal of Molecular Structure,* **1007:** 257-274.

18. N. Kar, M. Singh, R. Lal, (2012) Synthesis and spectral studies on heterobimetallic complexes of manganese and ruthenium derived from bis [N-(2-hydroxynaphthalen-1-yl) methylene] oxaloyldihydrazide, *Arabian Journal of Chemistry,* **5:** 67-72.

19. G. Svehla, (1979) *Vogel's Textbook of Macro and Semimicro Qualitative Inorganic Analysis,* London: Longman.

20. F. J. Welcher, (1958) Analytical uses of ethylenediaminetetraacetic acid, *Journal of the American Chemical Society,* **80:** 2600-2600.

126

21. A. Vogel, (1978) *A Text Book of Quantitative Inorganic Analysis,* London: ELBS.
22. B. Figgis, J. Lewis, R. Wilkins, (1960) *Modern Coordination Chemistry,* New York: Interscience.
23. V. Vichai, K. Kirtikara, (2006) Sulforhodamine B colorimetric assay for cytotoxicity screening, *Nature Protocols,* **1:** 1112-1116.
24. A. S. El-Tabl, M. M. E. W. Abd, M. A. Wahba, N. A. E. H. Abou-El-Fadl, (2015) Synthesis, characterization and anticancer activity of new metal complexes derived from 2-hydroxy-3-(hydroxyimino)-4-oxopentan-2-ylidene) benzohydrazide, *Bioinorganic Chemistry and Applications,* **2015:** 1-14.
25. W. J. Geary, (1971) The use of conductivity measurements in organic solvents for the characterisation of coordination compounds, *Coordination Chemistry Reviews,* **7:** 81-122.
26. K. K. Narang, V. P. Singh, (1993) Synthesis and characterization of cobalt (II), nickel (II), copper (II) and zinc (II) complexes with acetylacetone bis-benzoylhydrazone and acetylacetone bis-isonicotinoylhydrazone, *Transition Metal Chemistry,* **18:** 287-290.
27. O. Pouralimardan, A. C. Chamayou, C. Janiak, H. Hosseini-Monfared, (2007) Hydrazone Schiff base-manganese (II) complexes: Synthesis, crystal structure and catalytic reactivity, *Inorganica chimica acta,* **360,** 1599-1608.
28. R. Gup, B. Kırkan, (2005) Synthesis and spectroscopic studies of copper (II) and nickel (II) complexes containing hydrazonic ligands and heterocyclic coligand, *Spectrochimica Acta Part A: Molecular and Biomolecular Spectroscopy,* **62:** 1188-1195.
29. M. F. Fouda, M. M. Abd-Elzaher, M. M. Shakdofa, F. A. El-Saied, M. I. Ayad, A. S. El Tabl, (2008) Synthesis and characterization of a hydrazone ligand containing antipyrine and its transition metal complexes, *Journal of Coordination Chemistry,* **61:** 1983-1996.
30. M. Fouda, M. Abd-Elzaher, M. Shakdofa, F. El Saied, M. Ayad, A. El Tabl, (2008) Synthesis and characterization of transition metal complexes of N′-[(1, 5-dimethyl-3-oxo-2-phenyl-2, 3-dihydro-1H-pyrazol-4-yl) methylene] thiophene-2-carbohydrazide, *Transition Metal Chemistry,* **33:** 219-228.
31. G. Nagesh, B. Mruthyunjayaswamy, (2015) Synthesis, characterization and biological relevance of some metal (II) complexes with oxygen, nitrogen and oxygen (ONO) donor Schiff base ligand derived from thiazole and 2-hydroxy-1-naphthaldehyde, *Journal of Molecular Structure,* **1085:** 198-206.
32. K. B. Gudasi, M. S. Patil, R. S. Vadavi, R. V. Shenoy, S. A. Patil, M. Nethaji, (2006) X-ray crystal structure of the N-(2-hydroxy-1-naphthalidene) phenylglycine Schiff base.

33. M. R. Maurya, S. Khurana, C. Schulzke, D. Rehder, (2001) Dioxo-and oxovanadium (V) complexes of biomimetic hydrazone ONO donor ligands: Synthesis, characterisation, and reactivity, *European Journal of Inorganic Chemistry,* **2001:** 779-788.
34. I. Tossidis, C. Bolos, (1986) Monohalogenobenzoylhydrazones II. Synthesis and study of Ti (IV) complexes with monochlorobenzoylhydrazones of 2-furaldehyde, 2-thiophenaldehyde, 2-pyrrolaldehyde and di-2-pyridylketone as ligands, *Inorganica chimica acta,* **112:** 93-97.
35. M. Hong, H. Yin, X. Zhang, C. Li, C. Yue, S. Cheng, (2013) Di-and tri-organotin (IV) complexes with 2-hydroxy-1-naphthaldehyde 5-chloro-2-hydroxybenzoylhydrazone: Synthesis, characterization and *in vitro* antitumor activities, *Journal of Organometallic Chemistry,* **724:** 23-31.
36. M. R. Maurya, S. Agarwal, C. Bader, D. Rehder, (2005) Dioxovanadium (V) complexes of ONO donor ligands derived from pyridoxal and hydrazides: Models of vanadate-dependent haloperoxidases, *European Journal of Inorganic Chemistry,* **2005:** 147-157.
37. Z. A. El-Wahab, M. M. Mashaly, A. Salman, B. El-Shetary, A. Faheim, (2004) Co (II), Ce (III) and UO 2 (VI) bis-salicylatothiosemicarbazide complexes: Binary and ternary complexes, thermal studies and antimicrobial activity, *Spectrochimica Acta Part A: Molecular and Biomolecular Spectroscopy,* **60,** 2861-2873.
38. K. Nakamoto, (1986) *Infrared and Raman Spectra of Inorganic and Coordination Compounds,* New York: Wiley Online Library.
39. L. K. Gupta, U. Bansal, S. Chandra, (2007) Spectroscopic and physicochemical studies on nickel (II) complexes of isatin-3, 2′-quinolyl-hydrazones and their adducts, *Spectrochimica Acta Part A: Molecular and Biomolecular Spectroscopy,* **66:** 972-975.
40. A. S. El-Tabl, M. M. Shakdofa, A. M. Shakdofa, (2013) Metal complexes of N'-(2-hydroxy-5-phenyldiazenyl) benzylideneisonicotinohydrazide: Synthesis, spectroscopic characterization and antimicrobial activity, *Journal of the Serbian Chemical Society,* **78:** 39-55.
41. A. S. El-Tabl, M. M. Shakdofa, A. M. El-Seidy, A. N. Al-Hakimi, (2012) Synthesis, characterization and antifungal activity of metal complexes of 2-(5-((2-chlorophenyl) diazenyl)-2-hydroxybenzylidene) hydrazinecarbothioamide, *Phosphorus, Sulfur, and Silicon and the Related Elements,* **187:** 1312-1323.

42. S. Chandra, L. K. Gupta, (2005) Spectroscopic studies on Co (II), Ni (II) and Cu (II) complexes with a new macrocyclic ligand: 2, 9-dipropyl-3, 10-dimethyl-1, 4, 8, 11-tetraaza-5, 7: 12, 14-dibenzocyclotetradeca-1, 3, 8, 10-tetraene, *Spectrochimica Acta Part A: Molecular and Biomolecular Spectroscopy,* **61:** 1181-1188.

43. E. Saied, A. Fathy, M. M. Shakdofa, A. S. El Tabl, M. M. Abd Elzaher, (2014) Coordination behaviour of N′ 1, N′ 4-bis ((1, 5-dimethyl-3-oxo-2-phenyl-2, 3-dihydro-1H-pyrazol-4-yl) methylene) succinohydrazide toward transition metal ions and their antimicrobial activities, *Main Group Chemistry,* **13(2),** 87-103.

44. A. S. El-Tabl, (2002) Synthesis, characterisation and antimicrobial activity of manganese (II), nickel (II), cobalt (II), copper (II) and zinc (II) complexes of a binucleating tetradentate ligand, *Journal of Chemical Research,* **2002:** 529-531.

45. M. Aly, S. M. Imam, (1995) Characterization of copper (II), nickel (II), cobalt (II) and palladium (II) complexes of vicinal oxime-imine ligands; induced chelate isomerism in the same molecule of the nickel (II) complex, *Monatshefte für Chemie/Chemical Monthly,* **126:** 173-185.

46. A. B. P. Lever, (1968) *Inorganic Electronic Spectroscopy*, Amsterdam, Elsevier.

47. G. Q. Xiang, L. X. Zhang, A. J. Zhang, X. Q. Cai, M. L. Hu, (2004) 6-(2, 4-Difluorophenyl)-3-(3-methylphenyl)-7H-1, 2, 4-triazolo [3, 4-b][1, 3, 4] thiadiazine, *Acta Crystallographica Section E: Structure Reports Online,* **60,** 2249-2251.

48. R. Parihari, R. Patel, R. Patel, (2000) Synthesis and characterization of metal complexes of manganese-, cobalt-and zinc (II) with Schiff base and some neutral ligand, *Journal of The Indian Chemical Society,* **77:** 339-340.

49. S. Goel, S. Chandra, S. D. Dwivedi, (2013) Synthesis, spectral and biological studies of copper (II) and iron (III) complexes derived from 2-acetyl benzofuran semicarbazone and 2-acetyl benzofuran thiosemicarbazone, *Journal of Saudi Chemical Society*, Available online 23 July 2013, ISSN 1319-6103, http://dx.doi.org/10.1016/j.jscs.2013.07.005. (http://www.sciencedirect.com/science/article/pii/S1319610313000744).

50. N. El-wakiel, M. El-keiy, M. Gaber, (2015) Synthesis, spectral, antitumor, antioxidant and antimicrobial studies on Cu (II), Ni (II) and Co (II) complexes of 4-[(1H-Benzoimidazol-2-ylimino)-methyl]-benzene-1, 3-diol, *Spectrochimica Acta Part A: Molecular and Biomolecular Spectroscopy,* **147:** 117-123.

51. H. Krishna, C. Mahapatra, K. Dush, (1997) 4-, 5- and 6-coordinate complexes of copper (II) with substituted imidazoles original research articlejournal of inorganic and nuclear chemistry, *Dash J. Inorg. Nucl. Chem,* **39:** 1253-1258.

52. N. Thakkar, S. Bootwala, (1995) Synthesis and characterization of binuclear metal-complexes derived from some isonitrosoacetophenones and benzidine, *Indian Journal of Chemistry Section A-Inorganic Bio-Inorganic Physical Theoretical & Analytical Chemistry,* **34:** 370-374.

53. A. S. El-Tabl, S. A. El-Enein, (2004) Reactivity of the new potentially binucleating ligand, 2-(acetichydrazido-N-methylidene-α-naphthol)-benzothiazol, towards manganese (II), nickel (II), cobalt (II), copper (II) and zinc (II) salts, *Journal of Coordination Chemistry,* **57:** 281-294.

54. S. El-Tabla, M. M. E. Shakdofa and M. A. Whaba, (2015) Synthesis, characterization and fungicidal activity of binary and ternary metal(II) complexes derived from 4,4′-((4-nitro-1,2-phenylene) bis(azanylylidene))bis(3-(hydroxyimino)pentan-2-one)Spectrochimica Acta Part A: Molecular and Biomolecular Spectroscopy, 136, 1941-1949.

55. J. V. Mehta, S. B. Gajera, M. N. Patel, (2015) Antimalarial, antimicrobial, cytotoxic, DNA interaction and SOD like activities of tetrahedral copper (II) complexes, *Spectrochimica Acta Part A: Molecular and Biomolecular Spectroscopy,* **136:** 1881-1892.

56. B. Sarkar, G. Bocelli, A. Cantoni, A. Ghosh, (2008) Copper (II) complexes of symmetrical and unsymmetrical tetradentate Schiff base ligands incorporating 1-benzoylacetone: Synthesis, crystal structures and electrochemical behavior, *Polyhedron,* **27:** 693-700.

57. H. M. El-Tabl, F. A. El-Saied, M. I. Ayad, (2002) Manganese (II), iron (III), cobalt (II), nickel (II), copper (II), zinc (II), and uranyl (VI) complexes of n-(2-furylidene) benzothiazol-2-ylacet ohydrazide, *Synthesis and Reactivity in Inorganic and Metal-Organic Chemistry,* **32:** 1189-1203.

58. S. Chandra, L. K. Gupta, D. Jain, (2004) Spectroscopic studies on Mn (II), Co (II), Ni (II), and Cu (II) complexes with N-donor tetradentate (N 4) macrocyclic ligand derived from ethylcinnamate moiety, *Spectrochimica Acta Part A: Molecular and Biomolecular Spectroscopy,* **60,** 2411-2417.

59. A. S. El-Tabl, (2004) Synthesis and characterization of cobalt (II)/(III), nickel (II) and copper (II) complexes of new 14, 15 and 16-membered macrocyclic ligands, *Bulletin of the Korean Chemical Society,* **25:** 1757-1763.

60. A. El-Tabl, M. Shakdofa, A. El-Seidy, A.N.Al-Hakimi,(2011)Synthesis,characterization and biological studies of new Mn (II), Ni (II), Co (II), Cu (II) and Zn (II) of 2-(benzothiazol-2-yl)-N0-(25-dihydroxybenzylidene) acetohydrazide, *Journal of Korean Chemical Society,* **55:** 19-27.

61. H. El-Boraey, A. El-Tabl, (2003) Supramolecular copper (II) complexes with tetradentate ketoenamine ligands, *Polish Journal of Chemistry,* **77:** 1759-1775.

62. A. S. El-Tabl, (1997) An esr study of copper (II) complexes of N-hydroxyalkylsalicylideneimines, *Transition Metal Chemistry,* **23:** 63-65.

63. I. Procter, B. Hathaway, D. Billing, R. Dudley, P. Nicholls, (1969) Electronic energy levels and stereochemistry of the cis-distorted octahedral complex nitritobis-(2, 2′-bipyridyl) copper (II) nitrate, *Journal of the Chemical Society A: Inorganic, Physical, Theoretical,* 1192-1197.

64. D. Nikles, M. Powers, F. Urbach, (1983) Copper (II) complexes with tetradentate bis (pyridyl)-dithioether and bis (pyridyl)-diamine ligands. Effect of thio ether donors on the electronic absorption spectra, redox behavior, and EPR parameters of copper (II) complexes, *Inorganic Chemistry,* **22:** 3210-3217.

65. R. Ray, G. B. Kauffmann, (1990) An EPR study of copper (II)-substituted biguanide complexes. Part III, *Inorganica Chimica Acta,* **174:** 237-244.

66. D. Smith, (1970) Relationship between electron spin resonance g-values and covalent bonding in tetragonal copper (II) compounds, *Journal of the Chemical Society A: Inorganic, Physical, Theoretical,* 3108-3120.

67. A. S. El-Tabl, (2004) Synthetic and spectroscopic investigations of some transition metal complexes of hydroxy-oxime ligand, *Journal of Chemical Research,* **2004:** 19-22.

68. D. Kivelson, R. Neiman, (1961) ESR studies on the bonding in copper complexes, *The Journal of Chemical Physics,* **35:** 149-155.

69. A. N. Al-Hakimi, M. M. Shakdofa, A. M. El-Seidy, A. S. El-Tabl, (2011) N, N 2-bis (3-((3-hydroxynaphthalen-2-yl) methylene-amino) propyl) phthalamide, *Journal of the Korean Chemical Society,* **55(3):** 418-429.

70. M. Bhadbhade, D. Srinivas, (1993) Erratum to document cited in CA119 (26): 285036b, *Inorganic Chemistry,* **32:** 2458.

71. M. Symons, (1979) *Chemical and Biological Aspects of Electron Spin Resonance,* New York: Van Nostrand Reinhold Wokingham.

72. S. J. Shieh, C. M. Chea, S. M. Peng, (1992) A colorless Cu (II) complex of CuO6 with a compressed tetragonal octahedron, *Inorganica Chimica Acta,* **192:** 151-152.

73. A. El-Tabl, (1997) Synthesis and spectral studies on mononuclear copper (II) complexes of isonitrosoacetylacetone ligand, *Polish Journal of Chemistry,* **71:** 1213-1222.

74. A. S. El-Tabl, S. M. Imam, (1997) New copper (II) complexes produced by the template reaction of acetoacetic-2-pyridylamide and amino-aliphatic alcohols, *Transition Metal Chemistry,* **22:** 259-262.

75. M. Gaber, M. Ayad, M. Ayad, (1991) Synthesis, thermal and electrical studies on zirconyl complexes with schiff bases derived from 2-hydroxy-1-naphthaldehyde and some aromatic diamines, *Thermochimica Acta,* **176:** 21-29.

76. A. El-Tabl, M. Abou-Sekkina, (1999) Preparation and thermophysical properties of new cobalt (II), nickel (II) and copper (II) complexes, *Polish Journal of Chemistry,* **73:** 1937-1945.

77. N. A. Illán-Cabeza, A. R. García-García, M. N. Moreno-Carretero, J. M. Martínez-Martos, M. J. Ramírez-Expósito, (2005) Synthesis, characterization and antiproliferative behavior of tricarbonyl complexes of rhenium (I) with some 6-amino-5-nitrosouracil derivatives: Crystal structure of fac-[ReCl (CO) 3 (DANU-N 5, O 4)] (DANU= 6-amino-1, 3-dimethyl-5-nitrosouracil), *Journal of Inorganic Biochemistry,* **99:** 1637-1645.

78. I. H. Hall, C. C. Lee, G. Ibrahim, M. A. Khan, G. M. Bouet, (1997) Cytotoxicity of metallic complexes of furan oximes in murine and human tissue cultured cell lines, *Applied Organometallic Chemistry,* **11:** 565-575.

79. G. Feng, J. C. Mareque-Rivas, R. T. M. de Rosales, N. H. Williams, (2005) A highly reactive mononuclear Zn (II) complex for phosphodiester cleavage, *Journal of the American Chemical Society,* **127:** 13470-13471.

80. M. Gaetke, K. Chow, (2003) Copper toxicity, oxidative stress, and antioxidant nutrients, *Toxicology*, 189(1-2): 147–163.

81. C. Rouzer, (2010) Metals and DNA repair, *Chemical Research in Toxicology,* **23:** 1517-1518.

Bibliographical Sketch

Dr. A. S. Eltabl Inorganic chemistry, Ph. D Degree in 1993 from Menofya University. Joined as Assistant professor on 2000 and professor on 2009. More than 300 articles were published in national and international journals. Articles were presented in various national and international conferences. The current research activities include coordination Chemistry, metal complexes, and their biological activity applications